

## Monitoring the CMS endcap muon cathode strip chambers for aging

---

**Neha Rawal**<sup>a,\*</sup>

<sup>a</sup>*University of Florida,  
2001 Museum Rd, Gainesville FL, USA*

*E-mail:* [neha.rawal@ufl.edu](mailto:neha.rawal@ufl.edu), [neha.rawal@cern.ch](mailto:neha.rawal@cern.ch)

The Cathode Strip Chambers (CSCs) are multi-wire proportional chambers with cathode strip readout, and they constitute the primary muon tracking device in the endcaps of the CMS experiment at the LHC. The CSCs have accumulated a significant radiation dose since the beginning of LHC operations, and it is important to monitor any possible signs of aging and confirm that the detector can sustain the full expected integrated luminosity of the HL-LHC ( $3000 \text{ fb}^{-1}$ ). Aging effects are assessed by performing in-situ measurements of the gas gain in CSCs as a function of the integrated luminosity. Signs of aging could appear as a decreasing gas gain with increased integrated luminosity. CSC gas gain is studied using muon-induced charge on cathodes using data collected during 2022, corresponding to  $39.4 \text{ fb}^{-1}$ . The impact of atmospheric pressure and changes in detector settings (HV, gas mixture, etc.) are also taken into account.

\*\*\* LHC2023: The 11th annual conference on Large Hadron Collider Physics \*\*\*

\*\*\* 22-27 May 2023 \*\*\*

\*\*\* Belgrade, Serbia \*\*\*

---

\*Speaker

## 1. Introduction

Since the start of the LHC (Large Hadron Collider), the CSCs (Cathode Strip Chambers) have been exposed to a considerable amount of radiation. Considering the long term irradiation, we need to ensure that CSC chamber performance is not degrading, and they can sustain the full expected integrated luminosity of HL-LHC ( $3000 \text{ fb}^{-1}$ ) equivalent to an accumulated charge of  $200 \text{ mC/cm}$  [1]. Irradiation tests for CSC chamber longevity were performed at the CERN Gamma Irradiation Facility (GIF++) with full-scale CSC ME1/1, ME2/1 chambers. These chambers have been irradiated up to an accumulated charge equivalent to three times that expected at the maximum HL-LHC integrated luminosity [2], and no noticeable decrease in gas gain was observed. These accelerated aging studies suggest that CSCs will not suffer aging during the HL-LHC operation. Additionally for monitoring aging within these detectors, we can employ in-situ measurements of the gas gain in the CSCs. In this study, aging effects are assessed by monitoring in-situ gas gain as a function of the integrated luminosity.

## 2. The CSC detector in CMS

CSCs are multi-wire proportional chambers that constitute the primary muon tracking and triggering device in the CMS endcaps ( $0.9 \leq |\eta| \leq 2.4$ ) (Fig. 1a) [3]. Each CSC has six layers of anode wires and cathode strips with high voltage applied to the anode wire planes (Fig. 1b). A charged particle passing through the detector ionizes the gas mixture (40% Ar, 50% CO<sub>2</sub>, and 10% CF<sub>4</sub>). In the strong electric field, an avalanche of charged particles occurs around anode wires, providing radial measurement ( $r$ ), and an image charge is induced on the strips of cathode plane, providing azimuthal coordinate measurements ( $\phi$ ) (Fig. 1c). Combining position measurements from the cathode strips and anode wires provides a precise 2D hit position on each CSC layer.

There are 540 CSCs distributed among four stations per endcap. Station 1 has three rings of chambers while stations 2 to 4 each have two rings of chambers. The rings of chambers are designated by ME  $\pm$  S/R, where "ME" stands for "Muon Endcap", the  $\pm$  sign indicates the endcap, "S" indicates the disk (or "station") and "R" is the ring number. The chambers in the outer rings, such as ME  $\pm$  2/2 and ME  $\pm$  3/2, ME  $\pm$  4/2, covering  $10^\circ$  in  $\phi$ , are considerably larger than the chambers closer to the beam pipe. The chambers closer to the beamline such as ME  $\pm$  x/1 ( $x=1,2,3,4$ ), covering  $20^\circ$  in  $\phi$ , are subject to the highest particle rates. They are referred to as inner rings, while all the others are referred to as outer rings. Each of the chambers in the ME1/1 ring is further subdivided into two parts with separate readouts: ME1/1a, covering the region  $2.1 < |\eta| < 2.4$ , and ME1/1b, extending from  $|\eta| = 1.6$  to  $|\eta| = 2.1$ .

The CSCs have independent HV segments along the R direction (the distance to the beamline). There are 31 HV segment types, labelled MExyHVz, where x= Station (1-4), y=Ring (1-3), z=segment within a CSC (there are 1, 3, or 5 segments depending on chamber type with segment 1 being the innermost segment and progressively extending outwards to segment 5 as the outermost). Irradiation received by CSC chambers is uniform vs azimuthal angle, therefore, to assess longevity, gas gain is studied in these 31 HV segments averaged over each ring.

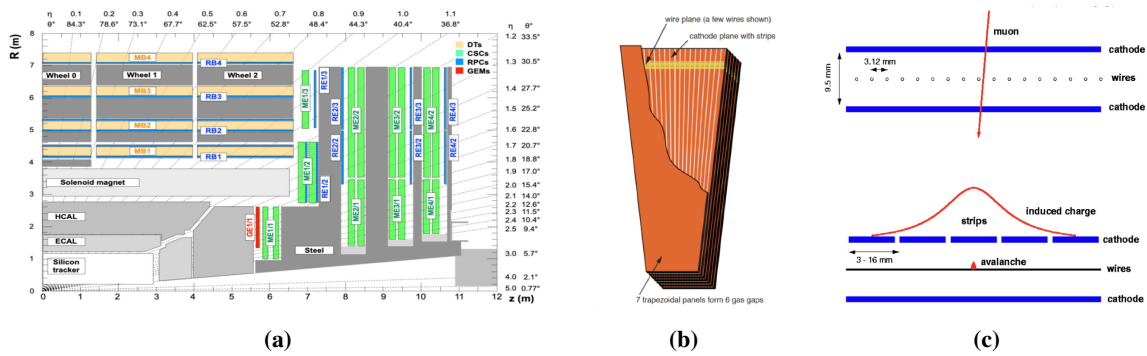


**Figure 1:** (a) Quarter view of CMS , (b) CSC chamber layout , (c) A schematic view of a single gap illustrating the principle of CSC operation

### 3. Analysis Overview

This analysis uses the dataset collected by CMS in 2022 during proton-proton collisions at  $\sqrt{s} = 13.6$  TeV corresponding to  $39.4 \text{ fb}^{-1}$  of integrated luminosity. Reconstructed CSC hits associated with  $Z \rightarrow \mu\mu$  events are selected if the event features a clear single muon track within the CSC, with a transverse momentum  $p_T > 10$  GeV, and compatible with the primary vertex [4].

The distribution of the induced muon charge in each HV segment displays a Landau shape as shown in Fig. 2 for ME21HV1. This charge distribution also includes contributions from spurious hits and saturation effects from electronics, which are removed by trimming off 30% of its tail, providing us induced muon charge. The truncated mean of this distribution gives us a proxy of the gas gain.

Gas gain is subject to variations influenced by several factors, including atmospheric pressure, HV changes during runs, changes in the gas mixture (e.g., changes in the proportion of Ar), the hit rate associated with instantaneous luminosity, and temperature fluctuations. In this analysis, the effects of some of these factors are considered step by step, and the relative gas gain trend is studied with integrated luminosity.

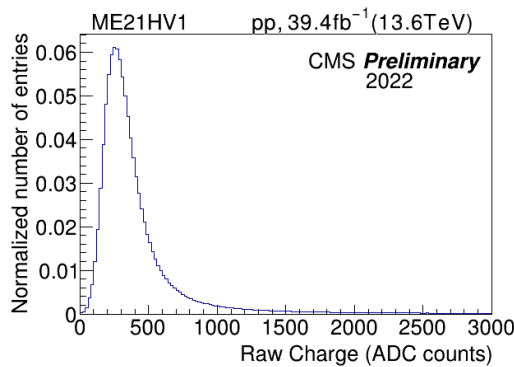


**Figure 2:** Charge distribution of reconstructed hits associated with ME21HV1 segment [4]

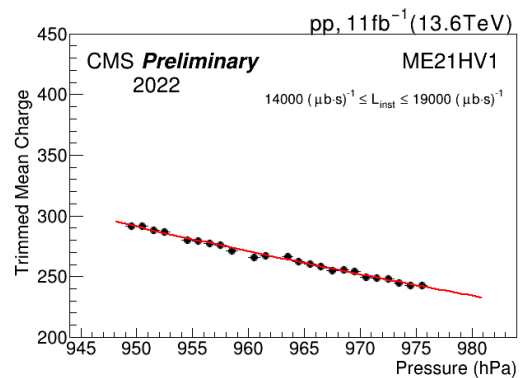


**Figure 3:** Gas gain dependence on atmospheric pressure for HV ME21HV segment. [4]

The gas gain dependency on atmospheric pressure was analyzed using data from an integrated

luminosity range of  $25 \text{ fb}^{-1} < \int \mathcal{L} dt < 36 \text{ fb}^{-1}$  and  $14000 (\mu\text{b}\cdot\text{s})^{-1} < L < 19000 (\mu\text{b}\cdot\text{s})^{-1}$  to factor out possible effects related to instantaneous/integrated luminosity variations. The atmospheric pressure dependence for individual HV segments is modeled with an exponential function,  $Q = \exp(a + bP)$ , as depicted in Fig. 3. The charge is then equalized to provide a gas gain across individual HV segments independent of pressure variations.  $Q_{\text{equalized charge}} = Q_{\text{raw}} \times \exp(-b \times (P - P_{\text{ref}}))$ .

Additionally, systematic effects on gas gain are mitigated by normalizing the gain of each HV segment to that of ME13HV3. Since ME13HV3 segment (outermost ring) receives low irradiation compared to other segments and so is expected not to be affected by aging, hence is used as a reference. This normalisation effectively cancels out any effects caused by unintended gas mixture variations.

#### 4. Results

The analysis presents a systematic procedure for in-situ study of aging in the CSC detectors. Removing gas gain dependence on atmospheric pressure and normalizing it relative to other chamber, we can see that ME2/1 chamber (Fig. 4a) remained stable within 5%. These variation is likely due to unaccounted systematic effects and is taken as an uncertainty in the measurement. Results for the other chamber types are very similar and the slope of gas gain versus integrated luminosity is shown (Fig. 4b) for all the chambers. This results indicate that there will be no relevant degradation of CSC performance when extrapolated to the integrated luminosity expected by the end of Run3 ( $300\text{fb}^{-1}$ ). To make definitive extrapolations toward the HL-LHC integrated luminosity, improved control over systematic effects is needed.

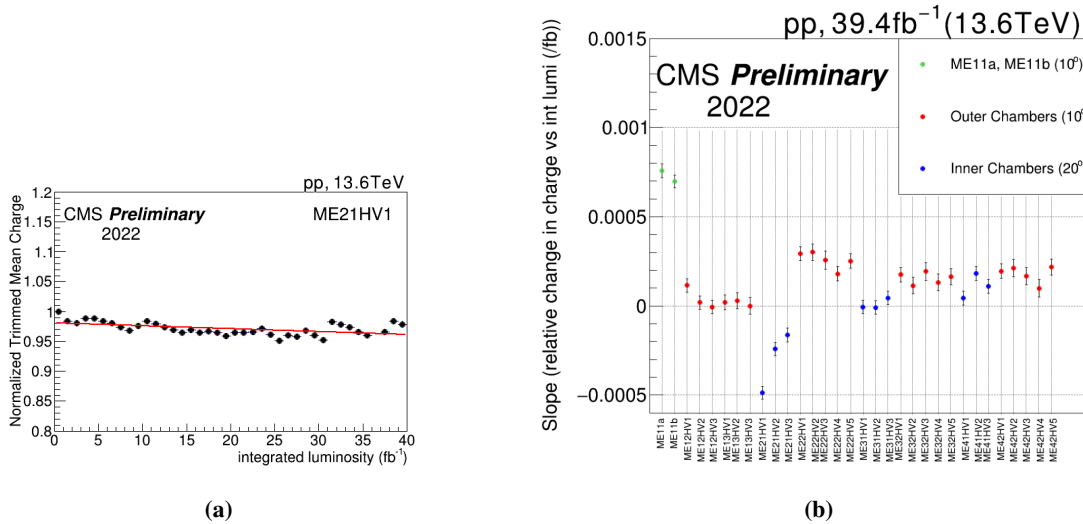


**Figure 4:** (a) Gas gain variation with integrated luminosity in ME21HV1 segments (b) Mean of Slope of gas gain dependence on integrated luminosity for different HV segments. [4]

## References

- [1] CMS Collaboration, *The Phase-2 Upgrade of the CMS Muon Detectors*, Tech. Rep. CERN-LHCC-2017-012, CMS-TDR-016, CERN, Geneva (2017).
- [2] Bingran Wang on behalf of the CMS muon group, *Longevity studies and Phase 2 electronics upgrade for CMS cathode strip chambers in preparation for HL-LHC*, NIM A 958 (2020), ISSN 0168-9002
- [3] Sirunyan, A. M. and others, The CMS Collaboration, *The CMS experiment at the CERN LHC*, JINST 3 S08004, 2008
- [4] Rawal N. and others, The CMS collaboration, *CSC gas gain stability monitoring using reconstructed hit charge: 2022*, CMS-DP-2023-058